Capacity Region of the Two-Way Multi-antenna Relay Channel with Analog Tx-Rx Beamforming

Cristian Lameiro, Alfredo Nazábal, Fouad Gholam, Javier Vía, and Ignacio Santamaría

Communications Engineering Department (DICOM), University of Cantabria, Santander, 39005, Spain
{lameiro,alfredo,fouad,jvia,nacho}@gtas.dicom.unican.es

Abstract. In this paper we study the multiple-input multiple-output two-way relay channel (MIMO-TWRC) when the nodes use analog beamforming. Following the amplify-and-forward (AF) strategy, the problem consists of finding the transmit and receive beamformers of the nodes and the relay, and the power allocated to each one, that achieve the boundary of the capacity region. We express the optimal node beamformers in terms of the relay beamformers, and show that the capacity region can be efficiently characterized using convex optimization techniques. Numerical examples are provided to illustrate the results of this paper, and to compare the capacity region achieved by analog beamforming against the conventional MIMO schemes that operate at the baseband.

Keywords: two-way relay channel, analog beamforming, convex optimization, capacity region.

1 Introduction

Analog beamforming has crescent interest due to the reduced cost, power consumption and system size in comparison to conventional multiple-input multiple-output (MIMO) schemes that apply beamforming in the digital domain [1]. Conventional MIMO systems require a radio-frequency (RF) chain for each antenna in order to process each data stream at baseband. On the other hand, applying beamforming in the RF domain (what we call hereafter RF-MIMO) entails acquiring and processing a single data stream, and thus the cost and power consumption are significantly reduced [2].

The RF-MIMO architecture is shown in Fig. 1. The transmitter (the receiver operates analogously) applies a set of complex weights, $w[n]$, which represent the gain factors and phase shifts at each antenna, and focus the energy beam in the proper direction. For point-to-point links, the design of the optimal Tx-Rx beamformers for multicarrier transmissions has been thoroughly considered in [2]-[4]. In [5], we proposed an optimal transmission strategy for the two-user RF-MIMO broadcast channel, and extended it to the K-user case and the multiple access channel.

On another front, cooperative and multihop communications have been a research topic of interest in recent years, due to the coverage extension that

J. Del Ser et al. (Eds.): MOBILIGHT 2011, LNICST 81, pp. 1–17, 2012.

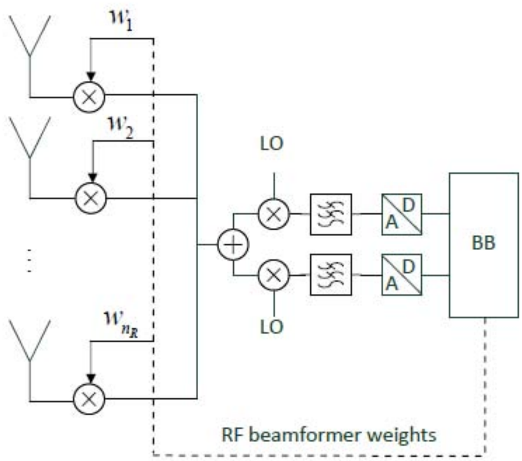

Fig. 1. RF-MIMO transceiver. A single data stream is processed, and thus the cost and power consumption are significantly reduced.

they provide. The two-way relay channel (TWRC) is one of the most basic multihop communication systems. The simplest TWRC consists of two source nodes that exchange information through an assisting relay node. We follow the coding strategy called amplify-and-forward (AF), also adopted in [6], [7]. Hence, only two phases are needed for the exchange of a whole data frame: a multiple access (MAC) phase and a broadcast (BC) phase.

Currently, the TWRC is receiving a great interest and there are many works on optimal transmission strategies and optimal beamforming for the multi-antenna case [6]-[9]. Authors in [6] consider the TWRC with amplify-and-forward (TWRC-AF) strategy when the source nodes are single antenna terminals and the relay uses conventional beamforming. They compute the optimal beamforming strategy at the relay node via convex optimization techniques with fixed powers, i.e., no power optimization is carried out. In [7], Wang and Zhang study the conventional MIMO-TWRC and propose a suboptimal method to compute the beamforming matrices. To the best of our knowledge, the MIMO-TWRC when the nodes use analog beamforming has not been considered yet in the literature. In this paper, we characterize the capacity region of the multi-antenna TWRC-AF, when all nodes use analog beamforming; what we call RF-TWRC. We show that the optimal beamforming strategy and the power allocation problem can be solved through efficient convex optimization techniques.

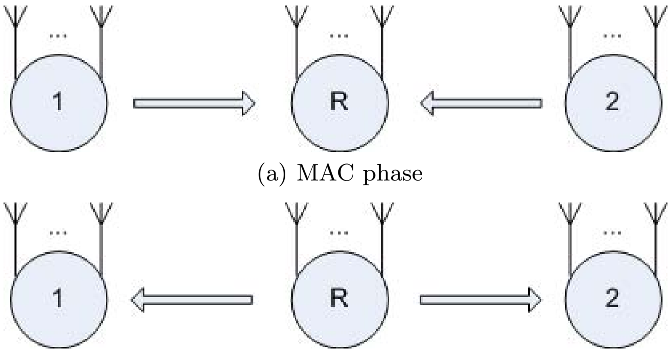

(a) MAC phase

(b) BC phase

Fig. 2. Two-way relay channel with amplify-and-forward strategy and two-phase protocol. In the MAC phase, the source nodes send their messages to the relay node; while in the BC phase, the relay node retransmits a linear composition of the received signal.

1.1 Notation

Bold upper and lower case letters denote matrices and vectors respectively; light-faced lower case letters denote scalar quantities. We use $\mathbf{A}^H$, $\mathbf{A}^*$ and $\mathbf{A}^T$ to denote Hermitian, conjugate and transpose of $\mathbf{A}$, respectively; $\mathrm{Tr}\,(\mathbf{A})$ denotes the trace of $\mathbf{A}$, and $\mathrm{rank}\,(\mathbf{A})$ denotes the rank of $\mathbf{A}$. For vectors, $\|\mathbf{a}\|$ denotes the Euclidean norm of $\mathbf{a}$; and for complex scalars, $|a|$ denotes the absolute value of a. The optimal solution of an optimization problem is indicated by $(\cdot)^{(*)}$.

2 System Model

We consider the TWRC depicted in Fig. 2, where two source nodes equipped with N_S antennas[1] establish a bidirectional communication through a relay node with N_R antennas. The two multi-antenna nodes and the relay perform beamforming in the RF domain, what it is called analog beamforming. We use the two-phase TWRC protocol which was also adopted in [6], [7]; and assume perfect channel state information at every node. In the MAC phase, both source nodes transmit simultaneously to the relay node. Due to the restrictions of the RF-MIMO architecture, the nodes are able to transmit a single data stream. Then, assuming flat-fading channels, the signal received at the relay node can be written as

$$\mathbf{y}_R = \mathbf{H}_1\mathbf{v}_1\sqrt{p_1}s_1 + \mathbf{H}_2\mathbf{v}_2\sqrt{p_2}s_2 + \mathbf{r}_R\ , \tag{1}$$

where $(\mathbf{v}_1, \mathbf{v}_2) \in \mathbb{C}^{N_S\times 1}$ are the unit-norm analog transmit beamformers of nodes 1 and 2, respectively; $(\mathbf{H}_1, \mathbf{H}_2) \in \mathbb{C}^{N_R\times N_S}$ are the channel matrices; and s_1 and s_2 are the symbols transmitted by nodes 1 and 2, respectively, which are assumed to be distributed as $CN(0, 1)$; p_1 and p_2 are the transmit powers of each source

[1] The extension to source nodes with different number of antennas is straightforward.

node; and $\mathbf{r}_R \sim CN(0, \sigma^2 \mathbf{I})$ represents the noise at the relay node. Note that, in contrast to [6], we consider multiple antennas at the nodes and the relay. In the BC phase, the relay node performs the amplify-and-forward strategy to linearly process the received signal (1). The analog beamforming matrix is

$$\mathbf{B} = \mathbf{v}_R \mathbf{u}_R^H \tag{2}$$

where $\mathbf{u}_R$ and $\mathbf{v}_R$ are the $N_R \times 1$ receive and transmit beamformers, respectively. Notice that, unlike [6], the RF-MIMO architecture imposes a rank-one constraint in the relay beamforming matrix (2).

Without loss of generality, we can assume $\|\mathbf{v}_R\|^2 = 1$ and $\|\mathbf{v}_i\|^2 = 1$, $i = 1, 2$. Thus, the transmit power of the relay node is given by

$$p_R(p_1, p_2, \mathbf{u}_R, \mathbf{v}_1, \mathbf{v}_2) = p_{\mathrm{ef}_1} + p_{\mathrm{ef}_2} + \sigma^2 \|\mathbf{u}_R\|^2 \tag{3}$$

where we have defined the effective power of source node i ($i = 1, 2$), p_{ef_i}, as

$$p_{\mathrm{ef}_i} = p_i \left|\mathbf{u}_R^H \mathbf{H}_i \mathbf{v}_i\right|^2, \qquad i = 1, 2 \ . \tag{4}$$

If channel reciprocity holds[2], i.e., the channels of source nodes 1 and 2 in the BC phase are $\mathbf{H}_1^T$ and $\mathbf{H}_2^T$, respectively; the signal received by the source nodes, after suppressing the self-interference, is

$$\begin{aligned} y_1 &= \mathbf{u}_1^H \mathbf{H}_1^T \mathbf{v}_R \sqrt{p_{\mathrm{ef}_2}} s_2 + \tilde{r}_1 \ , \\ y_2 &= \mathbf{u}_2^H \mathbf{H}_2^T \mathbf{v}_R \sqrt{p_{\mathrm{ef}_1}} s_1 + \tilde{r}_2 \ , \end{aligned} \tag{5}$$

where $\mathbf{u}_i \in \mathbb{C}^{N_s \times 1}$ and $\tilde{r}_i \sim CN\left(0, \sigma^2 \left[1 + \|\mathbf{u}_R\|^2 \left|\mathbf{u}_i^H \mathbf{H}_i^T \mathbf{v}_R\right|^2\right]\right)$ are the unit-norm analog receive beamformer and the equivalent noise at node i. Thus, the achievable bidirectional rate pairs, denoted by R_{12} (link from node 1 to node 2, through the relay node) and R_{21} (link from node 2 to node 1, through the relay node), are given by

$$R_{12} \leq \frac{1}{2} \log_2 \left[1 + \frac{p_{\mathrm{ef}_1} \left|\mathbf{u}_2^H \mathbf{H}_2^T \mathbf{v}_R\right|^2}{\sigma^2 \left(1 + \|\mathbf{u}_R\|^2 \left|\mathbf{u}_2^H \mathbf{H}_2^T \mathbf{v}_R\right|^2\right)}\right] , \tag{6}$$

$$R_{21} \leq \frac{1}{2} \log_2 \left[1 + \frac{p_{\mathrm{ef}_2} \left|\mathbf{u}_1^H \mathbf{H}_1^T \mathbf{v}_R\right|^2}{\sigma^2 \left(1 + \|\mathbf{u}_R\|^2 \left|\mathbf{u}_1^H \mathbf{H}_1^T \mathbf{v}_R\right|^2\right)}\right] . \tag{7}$$

In the next section, we derive the optimal beamforming vectors to be applied at the source nodes and define the capacity region of the MIMO RF-TWRC. Finally, we propose an iterative algorithm based on convex optimization techniques to compute the boundary of the capacity region.

[2] This assumption is made only for simplicity. The results hold also if different transmit and receive channels are considered.

3 Capacity Region

3.1 Optimal Node Beamformers and Parametrization

For a fixed transmit beamforming at the relay node, $\mathbf{v}_R$, the BC phase reduces to a single-input multiple-output (SIMO) channel. Thus, the optimal strategy for both nodes is matched filtering with respect to their channels or maximum ratio combining (MRC) [10]. Therefore, the unit-norm optimal analog receive beamformers are

$$\mathbf{u}_i = \frac{\mathbf{H}_i^T \mathbf{v}_R}{\left\|\mathbf{H}_i^T \mathbf{v}_R\right\|}, \qquad i = 1, 2 . \tag{8}$$

Similarly, for a fixed receive beamforming at the relay node, $\mathbf{u}_R$, the MAC phase reduces to a multiple-input single-output (MISO) channel. In order to achieve the boundary of the capacity region, each source node must control its effective power, p_{ef_i} $(i = 1, 2)$. According to (4), this power control can be done by varying either the source node power or its transmit beamformer, $\mathbf{v}_i$. Hence, if the source nodes perform maximum ratio transmission (MRT) [10], the effective power can be controlled solely by the source node power, p_i. Thus, MRT is always optimal. The MRT beamformers of the source nodes are given by

$$\mathbf{v}_i = \frac{\mathbf{H}_i^H \mathbf{u}_R}{\left\|\mathbf{H}_i^H \mathbf{u}_R\right\|}, \qquad i = 1, 2 . \tag{9}$$

In summary, the optimal Tx-Rx node beamformers can be written in terms of the Tx-Rx relay beamformers. Notice that, (8) and (9) implies that a feedback channel must exist between the nodes and the relay. According to that, the node beamformers can be computed at the relay node, and then sent them back to the nodes. With the optimal node beamformers, the rates in (6) and (7) can be rewritten as

$$R_{12} \leq \frac{1}{2} \log_2 \left[1 + \frac{p_{\mathrm{ef}_1} \left\|\mathbf{H}_2^T \mathbf{v}_R\right\|^2}{\sigma^2 \left(1 + \|\mathbf{u}_R\|^2 \left\|\mathbf{H}_2^T \mathbf{v}_R\right\|^2 \right)} \right] , \tag{10}$$

$$R_{21} \leq \frac{1}{2} \log_2 \left[1 + \frac{p_{\mathrm{ef}_2} \left\|\mathbf{H}_1^T \mathbf{v}_R\right\|^2}{\sigma^2 \left(1 + \|\mathbf{u}_R\|^2 \left\|\mathbf{H}_1^T \mathbf{v}_R\right\|^2 \right)} \right] , \tag{11}$$

where now $p_{\mathrm{ef}_i} = p_i \left\|\mathbf{H}_i^H \mathbf{u}_R\right\|^2$ $(i = 1, 2)$. Including the power constraints at the nodes and the relay, we can now define the capacity of the RF-TWRC as

$$C\left(P_1, P_2, P_R\right) \triangleq \bigcup_{p_1 \leq P_1, p_2 \leq P_2} \left[\bigcup_{\|\mathbf{v}_R\|^2 = 1, p_R(p_1, p_2, \mathbf{u}_R) \leq P_R} \left\{R_{12}, R_{21}\right\} \right] , \tag{12}$$

where R_{12} and R_{21} are defined in (10) and (11), respectively. It is easy to see that the optimal relay beamforming vectors must lie in the subspace spanned by the columns of the channel matrices, i.e.,

$$\begin{aligned} \mathbf{u}_R &\in \mathrm{span}\left(\mathbf{H}\right) \ , \\ \mathbf{v}_R &\in \mathrm{span}\left(\mathbf{H}^*\right) \ , \end{aligned} \tag{13}$$

where $\mathbf{H} = [\mathbf{H}_1, \mathbf{H}_2]$. Here, $\mathrm{span}\left(\mathbf{A}\right)$ denotes the subspace spanned by the columns of $\mathbf{A}$. Hence, taking the singular value decomposition (SVD) of $\mathbf{H}$, we can express the beamformers and the channel matrices in terms of a unitary basis as follows

$$\begin{aligned} \mathbf{u}_R &= \mathbf{U}\mathbf{a}_r \ , \\ \mathbf{v}_R &= \mathbf{U}^*\mathbf{a}_t \ , \\ \mathbf{H}_1 &= \mathbf{U}\mathbf{G}_1 \ , \\ \mathbf{H}_2 &= \mathbf{U}\mathbf{G}_2 \ , \end{aligned} \tag{14}$$

where $\mathbf{U} \in \mathbb{C}^{N_R \times \min(N_R, 2N_S)}$ is an orthogonal basis for the column range of $\mathbf{H}$. Vectors $\{\mathbf{a}_r, \mathbf{a}_t\} \in \mathbb{C}^{\min(N_R, 2N_S)\times 1}$ are the coefficients of the linear expansion of the beamformers in terms of the basis $\mathbf{U}$. As $\mathbf{U}$ is unitary, $\|\mathbf{v}_R\|^2 = 1$ implies $\|\mathbf{a}_t\|^2 = 1$. Note that, with this parametrization, the number of complex variables of $\mathbf{u}_R$ and $\mathbf{v}_R$ can be reduced from N_R to $2N_S$ if $N_R > 2N_S$.

With the parametrization given in (14), the rates achieved by the nodes are now given by

$$R_{12} \le \frac{1}{2}\log_2\left[1 + \frac{p_{\mathrm{ef}_1}\left\|\mathbf{G}_2^T\mathbf{a}_t\right\|^2}{\sigma^2\left(1 + \|\mathbf{a}_r\|^2\left\|\mathbf{G}_2^T\mathbf{a}_t\right\|^2\right)}\right] \ , \tag{15}$$

$$R_{21} \le \frac{1}{2}\log_2\left[1 + \frac{p_{\mathrm{ef}_2}\left\|\mathbf{G}_1^T\mathbf{a}_t\right\|^2}{\sigma^2\left(1 + \|\mathbf{a}_r\|^2\left\|\mathbf{G}_1^T\mathbf{a}_t\right\|^2\right)}\right] \ , \tag{16}$$

where now $p_{\mathrm{ef}_i} = p_i\left\|\mathbf{G}_i^H\mathbf{a}_r\right\|^2$ $(i = 1, 2)$. The capacity region is now given by

$$C\left(P_1, P_2, P_R\right) \triangleq \bigcup_{p_1 \le P_1, p_2 \le P_2}\left[\bigcup_{\|\mathbf{a}_t\|^2 = 1, p_R(p_1, p_2, \mathbf{a}_r) \le P_R}\{R_{12}, R_{21}\}\right] \ , \tag{17}$$

with R_{12} and R_{21} defined in (15) and (16), respectively.

3.2 Computing the Capacity Region

The capacity region in (17) can be characterized by solving a weighted sum-rate maximization problem (WSRmax). This approach assigns different weights to the source nodes in order to establish a priority between them. Hence, varying the weights, every point on the capacity boundary can be computed. However, the WSRmax problem is non-convex and it is very difficult to solve [11].

The authors of [12] proposed an alternative method to compute the boundary rate-tuples of the capacity region called *rate profile*, that was also applied in

[6] to the single-antenna TWRC. Applying this idea, the rate at each node can be expressed as a portion of the sum rate, i.e., $[R_{12}, R_{21}]^T = R_{\text{sum}} [\tau, 1-\tau]^T$, where $[\tau, 1-\tau]^T$ is the *rate profile* vector. Thus, for a fixed value of τ between 0 and 1, we can compute a boundary point of the capacity region by solving the following optimization problem

$$\begin{aligned} \underset{p_1,p_2,\mathbf{a}_t,\mathbf{a}_r,R_{\text{sum}}}{\text{maximize}} \quad & R_{\text{sum}} \ , \\ \text{subject to :} \ & \frac{1}{2}\log_2\left[1+\frac{p_1\left\|\mathbf{G}_1^H\mathbf{a}_r\right\|^2\left\|\mathbf{G}_2^T\mathbf{a}_t\right\|^2}{\sigma^2\left(1+\left\|\mathbf{a}_r\right\|^2\left\|\mathbf{G}_2^T\mathbf{a}_t\right\|^2\right)}\right] \geq \tau R_{\text{sum}} \ , \\ & \frac{1}{2}\log_2\left[1+\frac{p_2\left\|\mathbf{G}_2^H\mathbf{a}_r\right\|^2\left\|\mathbf{G}_1^T\mathbf{a}_t\right\|^2}{\sigma^2\left(1+\left\|\mathbf{a}_r\right\|^2\left\|\mathbf{G}_1^T\mathbf{a}_t\right\|^2\right)}\right] \geq (1-\tau) R_{\text{sum}} \ , \\ & p_1\left\|\mathbf{G}_1^H\mathbf{a}_r\right\|^2 + p_2\left\|\mathbf{G}_2^H\mathbf{a}_r\right\|^2 + \sigma^2\left\|\mathbf{a}_r\right\|^2 \leq P_R \ , \\ & p_1 \leq P_1 \ , \\ & p_2 \leq P_2 \ . \end{aligned} \tag{18}$$

SinceR_{12} and R_{21} grow monotonically with the signal-to-noise plus interference ratio (SINR), we can express the *rate profile* in terms of a *SINR profile*. Hence, for a fixed value of R_{sum}, the rate constraints in (18) are equivalent to target SINRs at the nodes, and thus the optimization problem (18) with fixed R_{sum} is equivalent to a power minimization problem with SINR constraints as follows

$$\begin{aligned} \underset{p_1,p_2,\mathbf{a}_t,\mathbf{a}_r}{\text{minimize}} \ & p_1\left\|\mathbf{G}_1^H\mathbf{a}_r\right\|^2 + p_2\left\|\mathbf{G}_2^H\mathbf{a}_r\right\|^2 + \sigma^2\left\|\mathbf{a}_r\right\|^2 \ , \\ \text{subject to :} \ & \frac{p_2\left\|\mathbf{G}_2^H\mathbf{a}_r\right\|^2\left\|\mathbf{G}_1^T\mathbf{a}_t\right\|^2}{\sigma^2\left(1+\left\|\mathbf{a}_r\right\|^2\left\|\mathbf{G}_1^T\mathbf{a}_t\right\|^2\right)} \geq \alpha\gamma_{\text{sum}} \ , \\ & \frac{p_1\left\|\mathbf{G}_1^H\mathbf{a}_r\right\|^2\left\|\mathbf{G}_2^T\mathbf{a}_t\right\|^2}{\sigma^2\left(1+\left\|\mathbf{a}_r\right\|^2\left\|\mathbf{G}_2^T\mathbf{a}_t\right\|^2\right)} \geq (1-\alpha)\gamma_{\text{sum}} \ , \\ & p_1 \leq P_1 \ , \\ & p_2 \leq P_2 \ , \end{aligned} \tag{19}$$

for some $0 \leq \alpha \leq 1$. For a given γ_{sum}, the solution of the above problem provides a feasible point of the capacity region if and only if $p_R^{(*)} \leq P_R$, where $p_R^{(*)}$ is the optimal power value. It turns out that the boundary of the capacity region can be obtained by a bisection method over γ_{sum}, solving problem (19) in each step, as indicated in algorithm 1.

Algorithm 1:

– **Initialize** $\gamma_{sum}^{min} = 0$, $\gamma_{sum}^{max} = \gamma_{sum}^{UB}$.
– **Repeat**

1. $\gamma_{sum} = \frac{1}{2}\left(\gamma_{sum}^{min} + \gamma_{sum}^{max}\right)$.
2. Solve problem (19).
   (a) If the problem is feasible, $\gamma_{sum}^{min} = \gamma_{sum}$.
   (b) Otherwise, $\gamma_{sum}^{max} = \gamma_{sum}$.

– **Until** $\left(\gamma_{sum}^{max} - \gamma_{sum}^{min}\right) \leq \epsilon$

A reasonable value of γ_{sum}^{UB} can be obtained through the SINR upper bound derived in [6]. This upper bound is obtained considering the optimal beamforming of both links independently. In the analog beamforming case, the optimal strategy at the relay node is transmitting and receiving through the principal eigenvectors of the channels. Hence, a SINR upper bound for the RF-TWRC is

$$\gamma_{sum}^{UB} = P_R\sigma_1^2\sigma_2^2\left(\frac{p_2}{P_R\sigma_1^2 + P_2\sigma_2^2 + \frac{1}{2}} + \frac{p_1}{P_R\sigma_2^2 + P_1\sigma_1^2 + \frac{1}{2}}\right) , \tag{20}$$

where σ_i is the strongest singular value of $\mathbf{G}_i$, $i = 1, 2$.

The optimization problem (19) is non-convex, but a solution can be found through a relaxed semidefinite programm (SDP), as we show in the next subsection.

3.3 Semidefinite Relaxation

Defining the Hermitian matrices $\mathbf{A}_r$ and $\mathbf{A}_t$ as

$$\begin{aligned}\mathbf{A}_r &= \mathbf{a}_r\mathbf{a}_r^H \ , \\ \mathbf{A}_t &= \mathbf{a}_t\mathbf{a}_t^H \ ,\end{aligned} \tag{21}$$

the optimization problem (19) can be written as

$$\begin{aligned}
\underset{p_1,p_2,\mathbf{A}_t,\mathbf{A}_r}{\text{minimize}} \quad & p_1\mathrm{Tr}\left(\mathbf{R}_1\mathbf{A}_r\right) + p_2\mathrm{Tr}\left(\mathbf{R}_2\mathbf{A}_r\right) + \sigma^2\mathrm{Tr}\left(\mathbf{A}_r\right) , \\
\text{subject to}: \ & p_2\mathrm{Tr}\left(\mathbf{R}_2\mathbf{A}_r\right) - (1-\alpha)\,\gamma_{\mathrm{sum}}\sigma^2\mathrm{Tr}\left(\mathbf{A}_r\right) \geq \frac{(1-\alpha)\,\gamma_{\mathrm{sum}}\sigma^2}{\mathrm{Tr}\left(\mathbf{R}_1^*\mathbf{A}_t\right)} , \\
& p_1\mathrm{Tr}\left(\mathbf{R}_1\mathbf{A}_r\right) - \alpha\gamma_{\mathrm{sum}}\sigma^2\mathrm{Tr}\left(\mathbf{A}_r\right) \geq \frac{\alpha\gamma_{\mathrm{sum}}\sigma^2}{\mathrm{Tr}\left(\mathbf{R}_2^*\mathbf{A}_t\right)} , \\
& \mathrm{Tr}\left(\mathbf{A}_t\right) = 1 , \\
& \mathbf{A}_t \succeq 0 , \\
& \mathbf{A}_r \succeq 0 , \\
& \mathrm{rank}\left(\mathbf{A}_t\right) = 1 , \\
& \mathrm{rank}\left(\mathbf{A}_r\right) = 1 , \\
& p_1 \leq P_1 , \\
& p_2 \leq P_2 ,
\end{aligned} \tag{22}$$

where $\mathbf{R}_i = \mathbf{G}_i\mathbf{G}_i^H$. The above problem can be shown to be still non-convex due to several reasons. First, the cross products between $\mathbf{A}_r$ and the power variables (p_1 and p_2) make the first two constraints non-convex. However, we can get through it by optimizing the effective powers instead. Thus, problem (22) is equivalent to

$$\begin{aligned}
\underset{p_{\mathrm{ef}_1}, p_{\mathrm{ef}_2}, \mathbf{A}_t, \mathbf{A}_r}{\text{minimize}} \quad & p_{\mathrm{ef}_1} + p_{\mathrm{ef}_2} + \sigma^2 \mathrm{Tr}\left(\mathbf{A}_r\right) , \\
\text{subject to}: \quad & p_{\mathrm{ef}_2} - (1-\alpha)\,\gamma_{\mathrm{sum}} \sigma^2 \mathrm{Tr}\left(\mathbf{A}_r\right) \geq \frac{(1-\alpha)\,\gamma_{\mathrm{sum}}\sigma^2}{\mathrm{Tr}\left(\mathbf{R}_1^* \mathbf{A}_t\right)} , \\
& p_{\mathrm{ef}_1} - \alpha \gamma_{\mathrm{sum}} \sigma^2 \mathrm{Tr}\left(\mathbf{A}_r\right) \geq \frac{\alpha\gamma_{\mathrm{sum}}\sigma^2}{\mathrm{Tr}\left(\mathbf{R}_2^* \mathbf{A}_t\right)} , \\
& \mathrm{Tr}\left(\mathbf{A}_t\right) = 1 , \\
& \mathbf{A}_t \succeq 0 , \\
& \mathbf{A}_r \succeq 0 , \\
& \mathrm{rank}\left(\mathbf{A}_t\right) = 1 , \\
& \mathrm{rank}\left(\mathbf{A}_r\right) = 1 , \\
& p_{\mathrm{ef}_1} \leq P_1 \mathrm{Tr}\left(\mathbf{R}_1 \mathbf{A}_r\right) , \\
& p_{\mathrm{ef}_2} \leq P_2 \mathrm{Tr}\left(\mathbf{R}_2 \mathbf{A}_r\right) .
\end{aligned} \tag{23}$$

Note that the last two inequalities are the power constraints of the source nodes, according to the definition of the effective powers in (4). On the other hand, the rank-one constraints are non-convex, although we can find a solution relaxing these two constraints, what is called in the literature a relaxed SDP, as we show in the following.

$$\begin{aligned}
\underset{p_{\mathrm{ef}_1}, p_{\mathrm{ef}_2}, \mathbf{A}_t, \mathbf{A}_r}{\text{minimize}} \quad & p_{\mathrm{ef}_1} + p_{\mathrm{ef}_2} + \sigma^2 \mathrm{Tr}\left(\mathbf{A}_r\right) , \\
\text{subject to}: \quad & p_{\mathrm{ef}_2} - (1-\alpha)\,\gamma_{\mathrm{sum}} \sigma^2 \mathrm{Tr}\left(\mathbf{A}_r\right) \geq \frac{(1-\alpha)\,\gamma_{\mathrm{sum}}\sigma^2}{\mathrm{Tr}\left(\mathbf{R}_1^* \mathbf{A}_t\right)} , \\
& p_{\mathrm{ef}_1} - \alpha \gamma_{\mathrm{sum}} \sigma^2 \mathrm{Tr}\left(\mathbf{A}_r\right) \geq \frac{\alpha\gamma_{\mathrm{sum}}\sigma^2}{\mathrm{Tr}\left(\mathbf{R}_2^* \mathbf{A}_t\right)} , \\
& \mathrm{Tr}\left(\mathbf{A}_t\right) = 1 , \\
& \mathbf{A}_t \succeq 0 , \\
& \mathbf{A}_r \succeq 0 , \\
& p_{\mathrm{ef}_1} \leq P_1 \mathrm{Tr}\left(\mathbf{R}_1 \mathbf{A}_r\right) , \\
& p_{\mathrm{ef}_2} \leq P_2 \mathrm{Tr}\left(\mathbf{R}_2 \mathbf{A}_r\right) .
\end{aligned} \tag{24}$$

The above problem is convex and can be efficiently solved using convex optimization methods. Moreover, as we show in the Appendix following the lines in [13], [14]; when the rank of the optimal beamforming matrices, $\mathbf{A}_t^{(*)}$ and $\mathbf{A}_r^{(*)}$, is greater than one, we are able to find an optimal rank-one solution. Thus, the solution of (24) is also the optimal solution of the original problem (19). Given the solution of (24), the optimal power assigned to each source node, $p_1^{(*)}$ and $p_2^{(*)}$, are given by

$$p_1^{(*)} = \frac{p_{\text{ef}_1}^{(*)}}{\text{Tr}\left(\mathbf{R}_1\mathbf{A}_r^{(*)}\right)}, \tag{25}$$

$$p_2^{(*)} = \frac{p_{\text{ef}_2}^{(*)}}{\text{Tr}\left(\mathbf{R}_2\mathbf{A}_r^{(*)}\right)}.$$

Note that, in contrast to [6], we are able to optimize the power of each source node and thus characterize completely the capacity region of the RF-TWRC, without resorting to an exhaustive search on the transmit powers.

4 Numerical Examples

In this section, we present some examples to illustrate the results of this paper, and to compare the achievable rates of the analog beamforming architecture with those achieved by conventional MIMO schemes. The elements of $\mathbf{H}_1$ and $\mathbf{H}_2$ are i.i.d. zero-mean circular complex Gaussian random variables with unit variance. We consider equal power constraints for the nodes and the relay, i.e., $P_R = P_1 = P_2 = P$, and define the signal-to-noise ratio as $\text{SNR} = 10\log_{10}\frac{P}{\sigma^2}$. Without loss of generality, we take $\sigma^2 = 1$. To get the boundary of the capacity region, we follow Algorithm 1 varying α between 0 and 1.

4.1 Conventional MIMO vs. Analog Beamforming

In this subsection we compare the achievable rate region when the nodes use analog beamforming against the conventional (baseband) MIMO beamforming. The capacity region with conventional MIMO is obtained through the algorithm proposed in [6]. This algorithm does not allow power optimization and requires the source nodes to be single antenna terminals. Thus, we focus on the following scenario: $N_s = 1$, $N_R = 4$ and fixed powers.

For convenience of the analysis, we consider one channel realization of $\mathbf{h}_1$ normalized by its own norm. Channel vector $\mathbf{h}_2$ is obtained such that $\|\mathbf{h}_2\| = 1$ and $\left|\mathbf{h}_1^H\mathbf{h}_2\right|^2 = \rho$, where ρ, $0 \leq \rho \leq 1$, is the squared cosine of the angle formed between $\mathbf{h}_1$ and $\mathbf{h}_2$.

Fig. 3(a) and Fig. 3(b) show the achievable rate region of both schemes for $\rho = 0.1$ and $\rho = 0.5$, respectively. The SNR is equal to 10 dB and the relay node is equipped with 4 antennas. As ρ increases, the channel vectors tend to be collinear and the gap between analog and conventional beamforming goes to 0.

4.2 Capacity Region of RF-TWRC

In this subsection we consider multi-antenna nodes and optimize the power transmitted by the source nodes. In Fig. 4 we show the capacity region of a RF-TWRC channel, when $N_R = 4$ and $N_S = 2$; and in Fig. 5 we show the power used by

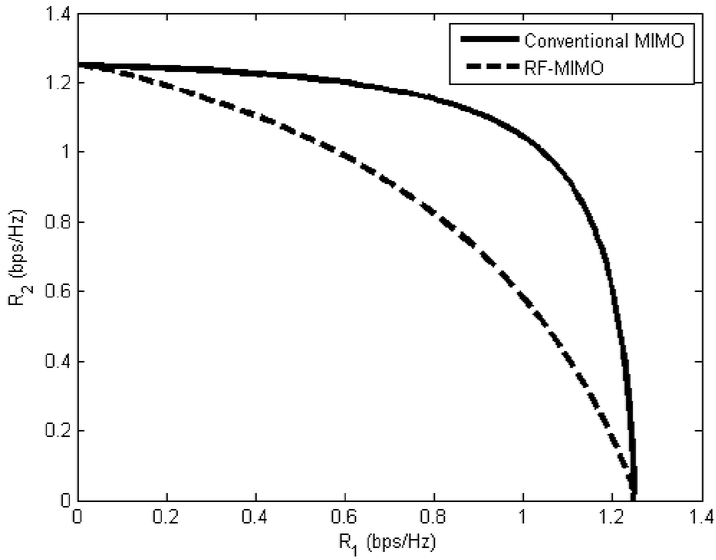

(a) $\rho = 0.1$

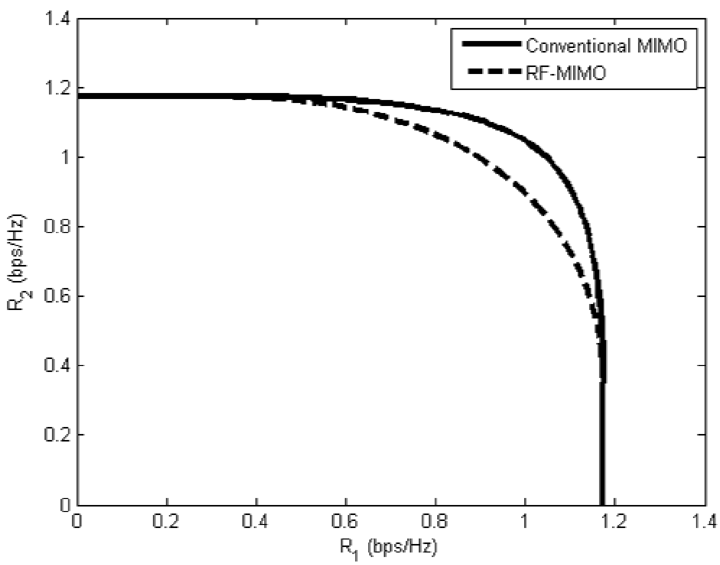

(b) $\rho = 0.5$

Fig. 3. Comparison between the achievable rates of conventional MIMO and RF-MIMO schemes when $N_s = 1$ and $N_R = 4$, for different values of ρ. The capacity of conventional MIMO-TWRC has been computed using the algorithm proposed in [6]. As ρ increases (i.e., more collinear channels), the gap between both regions tends to 0.

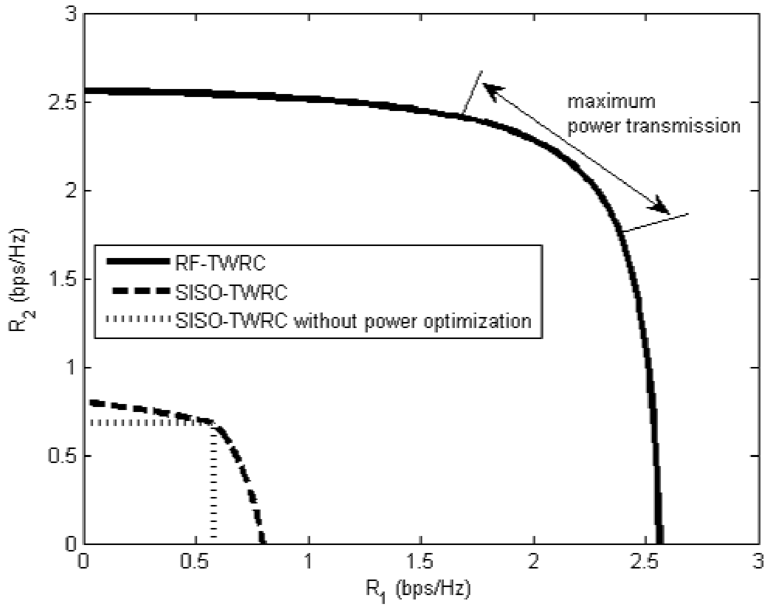

Fig. 4. Capacity region of the 4x2 RF-TWRC with a SNR of 10 dB. The dashed line depicts the achievable region of the SISO case with and without power optimization.

the source nodes. The SNR has a value of 10 dB and the energies of the channels are equal to unity. We observe that there are some points of the boundary that are achieved when the source nodes do not transmit at maximum power. This result can be easily explained in terms of the transmit power of the relay node, p_R. From (3), p_R is a function of the effective powers of both source nodes. As the relay node has a power constraint, P_R, the greater is the effective power of a node, the lower is the effective power of the other. To better understand this idea, consider one of the extreme points of the capacity boundary. If we fix $\alpha = 0$, i.e., full priority is assigned to node 1, then the optimal power of node 1, $p_1^{(*)}$, is equal to 0; while the optimal power of node 2, $p_2^{(*)}$, is maximized. As α increases, $p_1^{(*)}$ increases too, until it reaches its maximum value. Thus, maximum power transmission is optimal only in a subset of the capacity boundary.

Fig. 4 also shows the capacity region of the single antenna (SISO) case using the first antenna of each terminal, with and without power optimization (in the later case, both nodes always transmit at maximum power). We clearly observe the enlargement of the capacity region when the nodes are multi-antenna terminals performing analog beamforming. Moreover, optimizing the power of the source nodes noticeably improves the capacity region of the SISO-TWRC.

Similarly to the previous subsection, we also study the impact of the collinearity between the channels, that can be measured through the squared cosine of

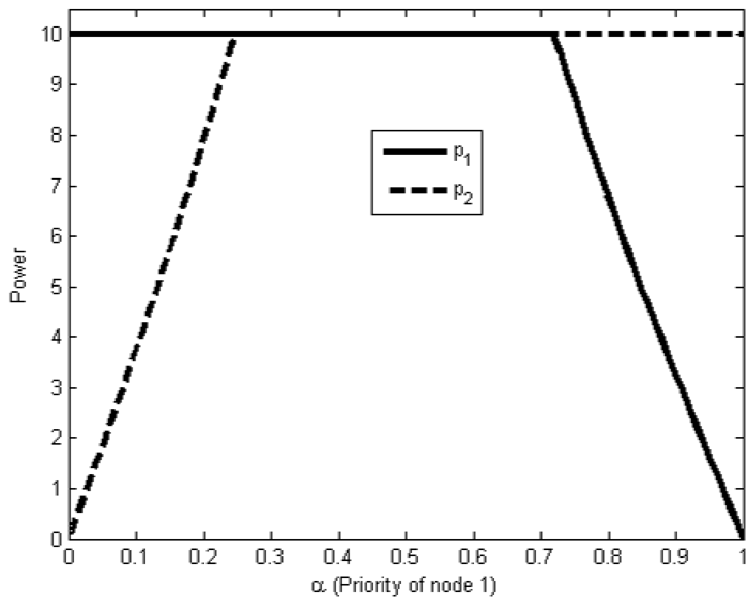

Fig. 5. Power allocation of the 4x2 RF-TWRC with a SNR of 10 dB. Note that only a subset of the boundary rate-tuples are achieved when both nodes are simultaneously transmitting at maximum power. Moreover, there is at least one node transmitting at maximum power at each boundary point.

the angle formed between them, ρ, that we compute using the Matlab function subspace(). For the convenience of the analysis, we normalize each channel by its own 2-norm. Fig. 6 shows the capacity of the RF-TWRC for different values of ρ, when $N_R = 4$, $N_S = 2$ and the SNR is 10 dB. As in the single-antenna case, the capacity region increases when the angle between the channels decreases.

4.3 Sum-Rate vs. SNR Analysis

In this subsection we evaluate the sum-rate capacity versus the SNR of the RF-TWRC through Monte Carlo simulation (specifically, we average the results of 100 channel realizations) and compare it with the conventional MIMO-TWRC and the SISO case, when the first antenna of each terminal is used. The sum-rate capacity is computed using exhaustive search over α, and we follow the algorithm proposed in [6] for the conventional MIMO-TWRC. Thus, we consider single antenna nodes, i.e., $N_S = 1$, and no power optimization, i.e, $p_1 = p_2 = P$. Fig. 7 shows the sum-rate capacity when the relay is equipped with $N_R = 4$ antennas. We observe that the RF-TWRC and the conventional MIMO-TWRC perform closely, as well as the enlargement in the sum-rate capacity with respect to the SISO case.

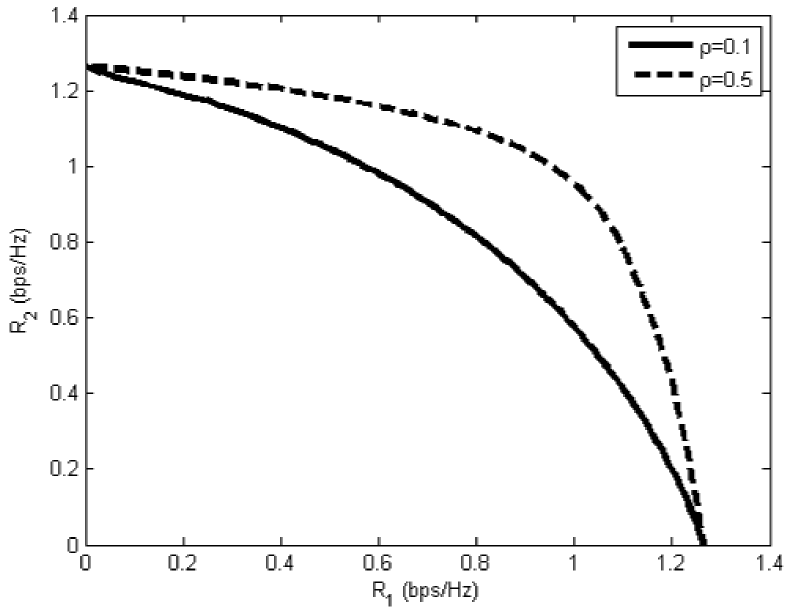

Fig. 6. Capacity region of the 4x2 RF-TWRC with a SNR of 10 dB, and different values of ρ. As ρ increases, the channels tend to be collinear and the capacity region increases.

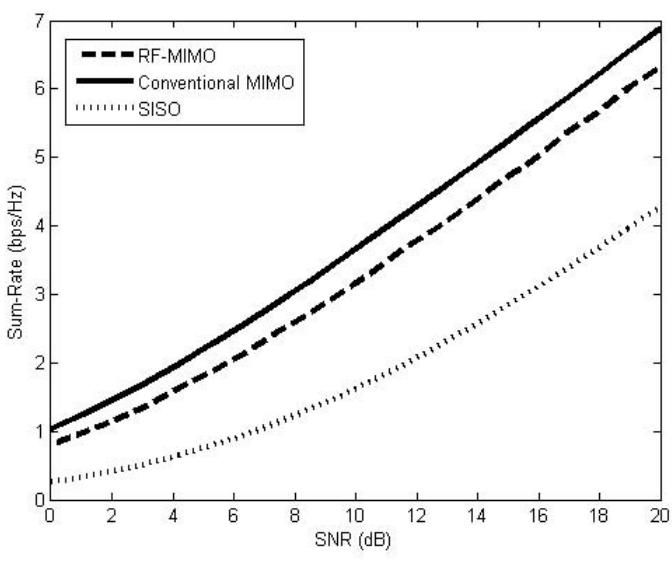

Fig. 7. Sum-rate capacity through Monte Carlo simulation (specifically, we average the results of 100 channel realizations) for the TWRC channel with $N_R = 4$ and $N_S = 1$, when no power optimization is performed.

5 Conclusions

RF-MIMO transceivers that apply beamforming in the analog domain are of practical interest due to the reduced system size, cost and power consumption in comparison with the conventional MIMO architectures. In this paper we have studied a basic TWRC-AF, when the two nodes and the relay are RF-MIMO terminals. Our main contribution has been to show that the optimal beamforming vectors and the power allocation can be efficiently computed using convex optimization techniques, through an iterative algorithm based on a bisection method. We have also shown that the capacity gap between analog beamforming and conventional MIMO schemes, when the source nodes are single antenna terminals and no power optimization is performed, goes towards 0 as the correlation coefficient between the channels increases.

A Appendix I

Suppose that the optimal solution of (24), $\mathbf{A}_r^{(*)}$, has rank $r > 1$. If there exists an equivalent rank-one solution, the following must hold

$$\begin{aligned}\mathrm{Tr}\left(\mathbf{R}_1\tilde{\mathbf{A}}_r\right) &= \mathrm{Tr}\left(\mathbf{R}_1\mathbf{A}_r^{(*)}\right) ,\\ \mathrm{Tr}\left(\mathbf{R}_2\tilde{\mathbf{A}}_r\right) &= \mathrm{Tr}\left(\mathbf{R}_2\mathbf{A}_r^{(*)}\right) ,\\ \mathrm{Tr}\left(\tilde{\mathbf{A}}_r\right) &= \mathrm{Tr}\left(\mathbf{A}_r^{(*)}\right) ,\end{aligned} \tag{26}$$

where $\tilde{\mathbf{A}}_r$ is a rank-one matrix. Through the matrix decomposition theorem for Hermitian matrices [13], [14]; given the Hermitian matrices $\mathbf{R}_1$ and $\mathbf{R}_2$, there exists a decomposition of $\mathbf{A}_r^{(*)}$, $\mathbf{A}_r^{(*)} = \sum_{k=1}^{r} \mathbf{a}_r^{(k)} \left(\mathbf{a}_r^{(k)}\right)^H$, such that,

$$\begin{aligned}\mathrm{Tr}\left(\mathbf{R}_1\tilde{\mathbf{A}}_r^{(k)}\right) &= \mathrm{Tr}\left(\mathbf{R}_1\mathbf{A}_r^{(*)}\right) ,\\ \mathrm{Tr}\left(\mathbf{R}_2\tilde{\mathbf{A}}_r^{(k)}\right) &= \mathrm{Tr}\left(\mathbf{R}_2\mathbf{A}_r^{(*)}\right) ,\end{aligned} \tag{27}$$

for all $k = 1, \ldots, r$; where $\tilde{\mathbf{A}}_r^{(k)} = r\mathbf{a}_r^{(k)} \left(\mathbf{a}_r^{(k)}\right)^H$ is a rank-one matrix. Thus, there exist r rank-one matrices that satisfy the first two conditions in (26). Taking into account that the trace of $\mathbf{A}_r^{(*)}$ and $\tilde{\mathbf{A}}_r^{(k)}$ are, respectively, given by

$$\begin{aligned}\mathrm{Tr}\left(\mathbf{A}_r^{(*)}\right) &= \sum_{k=1}^{r} \left\|\mathbf{a}_r^{(k)}\right\|^2 ,\\ \mathrm{Tr}\left(\tilde{\mathbf{A}}_r^{(k)}\right) &= r\left\|\mathbf{a}_r^{(k)}\right\|^2 ,\end{aligned} \tag{28}$$

and assuming without loss of generality, $\left\|\mathbf{a}_r^{(1)}\right\|^2 \geq \left\|\mathbf{a}_r^{(2)}\right\|^2 \geq \ldots \geq \left\|\mathbf{a}_r^{(r)}\right\|^2$; it follows that

$$\mathrm{Tr}\left(\mathbf{A}_r^{(*)}\right) \geq \mathrm{Tr}\left(\tilde{\mathbf{A}}_r^{(r)}\right) . \tag{29}$$

On the other hand, as $\mathbf{A}_r^{(*)}$ is an optimal solution of (24), the following must hold

$$\mathrm{Tr}\left(\mathbf{A}_r^{(*)}\right) \leq \mathrm{Tr}\left(\tilde{\mathbf{A}}_r^{(r)}\right) . \tag{30}$$

Thus, to satisfy (29) and (30), both traces must be equal, i.e.,

$$\mathrm{Tr}\left(\mathbf{A}_r^{(*)}\right) = \mathrm{Tr}\left(\tilde{\mathbf{A}}_r^{(r)}\right) . \tag{31}$$

Therefore, the rank-one matrix $\tilde{\mathbf{A}}_r^{(r)}$ is also optimal and equivalent to $\mathbf{A}_r^{(*)}$.

Similarly, suppose that the optimal solution of (24), $\mathbf{A}_t^{(*)}$, has rank $r > 1$. If there exists an equivalent rank-one solution, the following must hold

$$\begin{aligned} \mathrm{Tr}\left(\mathbf{R}_1^*\tilde{\mathbf{A}}_t\right) &= \mathrm{Tr}\left(\mathbf{R}_1^*\mathbf{A}_t^{(*)}\right) , \\ \mathrm{Tr}\left(\mathbf{R}_2^*\tilde{\mathbf{A}}_t\right) &= \mathrm{Tr}\left(\mathbf{R}_2^*\mathbf{A}_t^{(*)}\right) , \\ \mathrm{Tr}\left(\tilde{\mathbf{A}}_t\right) &= \mathrm{Tr}\left(\mathbf{A}_t^{(*)}\right) , \end{aligned} \tag{32}$$

where $\tilde{\mathbf{A}}_t$ is a rank-one matrix. The above conditions are equivalent to (26), and the same arguments can be invoked to prove the existence of an optimal rank-one matrix.

Acknowledgment. The research leading to these results has received funding from the European Community's Seventh Framework Programme (FP7/2007-2013) under grant agreement n 213952, MIMAX and by the Spanish Government (MICINN) under projects TEC2007-68020-C04-02/TCM (MULTIMIMO) and TEC2010-19545-C04-03 (COSIMA).

References

1. Eickhoff, R., Kraemer, R., Santamaría, I., González, L.: Developing energy-efficient MIMO radios. IEEE Vehicular Technology Magazine 4(1), 34–41 (2009)
2. Vía, J., Elvira, V., Santamaría, I., Eickhoff, R.: Analog antenna combining for maximum capacity under OFDM transmissions. In: Proceedings of the 2009 IEEE International Conference on Communications, Dresden, Germany, pp. 3129–3133 (2009)
3. Vía, J., Santamaría, I., Elvira, V., Eickhoff, R.: A general criterion for analog Tx-Rx beamforming under OFDM transmissions. IEEE Transactions on Signal Processing 58(4), 2155–2167 (2010)
4. Vía, J., Elvira, V., Santamaría, I., Eickhoff, R.: Minimum BER beamforming in the RF domain for OFDM transmissions and linear receivers. In: IEEE International Conference on Acoustics Speech and Signal Processing (ICASSP 2009), Taipei, Taiwan (March 2009)
5. Santamaría, I., Vía, J., Nazábal, A., Lameiro, C.: Capacity region of the multi-antenna gaussian broadcast channel with analog Tx-Rx beamforming. In: 5th International ICST Conference on Communications and Networking in China (CHINACOM), Beijing, China (August 2010)

6. Zhang, R., Liang, Y.-C., Chai, C.C., Cui, S.: Optimal beamforming for two-way multi-antenna relay channel with analogue network coding. IEEE Journal on Selected Areas in Communications 27(5), 699–712 (2009)
7. Wang, X., Zhang, X.-D.: Optimal beamforming in MIMO two-way relay channels. In: IEEE Global Communications Conference (GLOBECOM 2010), Miami, FL, USA (December 2010)
8. Wyrembelski, R.F., Oechtering, T.J., Boche, H.: MIMO bidirectional broadcast channels with common message. In: IEEE Global Communications Conference (GLOBECOM 2010), Miami, FL, USA (December 2010)
9. Oechtering, T., Wyrembelski, R., Boche, H.: Multiantenna bidirectional broadcast channels - optimal transmit strategies. IEEE Transactions on Signal Processing 57(5), 1948–1958 (2009)
10. Tse, D., Viswanath, P.: Fundamentals of Wireless Communications. Cambridge University Press (2004)
11. Boyd, S., Vandenberghe, L.: Convex Optimization. Cambridge University Press (2004)
12. Mohseni, M., Zhang, R., Cioffi, J.: Optimized transmission for fading multiple-access and broadcast channels with multiple antennas. IEEE Journal on Selected Areas in Communications 24(8), 1627–1639 (2006)
13. Huang, Y., Zhang, S.: Complex matrix decomposition and quadratic programming. Math. Oper. Res. 32, 758–768 (2007)
14. Palomar, D., Eldar, Y.: Convex Optimization in Signal Processing and Communications. Cambridge University Press (2010)